American College of Neuropsychopharmacology

www.nature.com/npp

ARTICLE

Check for updates

Dynamic activity of interpeduncular nucleus GABAergic neurons controls expression of nicotine withdrawal in male mice

Paul M. Klenowski[1,2]✉, Rubing Zhao-Shea[1,2], Timothy G. Freels[1], Susanna Molas[1] and Andrew R. Tapper[1]✉

A critical brain area implicated in nicotine dependence is the interpeduncular nucleus (IPN) located in the ventral midbrain and consisting primarily of GABAergic neurons. Previous studies indicate that IPN GABAergic neurons contribute to expression of somatic symptoms of nicotine withdrawal; however, whether IPN neurons are dynamically regulated during withdrawal in vivo and how this may contribute to both somatic and affective withdrawal behavior is unknown. To bridge this gap in knowledge, we expressed GCaMP in IPN GABAergic neurons and used in vivo fiber photometry to record changes in fluorescence, as a proxy for neuronal activity, in male mice during nicotine withdrawal. Mecamylamine-precipitated withdrawal significantly increased activity of IPN GABAergic neurons in nicotine-dependent, but not nicotine-naive mice. Analysis of GCaMP signals time-locked with somatic symptoms including grooming and scratching revealed reduced IPN GABAergic activity during these behaviors, specifically in mice undergoing withdrawal. In the elevated plus maze, used to measure anxiety-like behavior, an affective withdrawal symptom, IPN GABAergic neuron activity was increased during open-arm versus closed-arm exploration in nicotine-withdrawn, but not non-withdrawn mice. Optogenetic silencing IPN GABAergic neurons during withdrawal significantly reduced withdrawal-induced increases in somatic behavior and increased open-arm exploration. Together, our data indicate that IPN GABAergic neurons are dynamically regulated during nicotine withdrawal, leading to increased anxiety-like symptoms and somatic behavior, which inherently decrease IPN GABAergic neuron activity as a withdrawal-coping mechanism. These results provide a neuronal basis underlying the role of the IPN in the expression of somatic and affective behaviors of nicotine withdrawal.

Neuropsychopharmacology (2022) 47:641–651; https://doi.org/10.1038/s41386-021-01107-1

INTRODUCTION

Nicotine is a highly addictive tertiary alkaloid found in tobacco [1, 2]. The consumption of nicotine from smoking causes 480,000 deaths each year in the US [3] and accounts for healthcare costs and workplace losses totaling more than $300 billion annually [3, 4]. Despite the negative consequences of smoking including increased risk of adverse health events and reduced life expectancy, smokers often find it difficult to reduce their intake [5]. This is largely due to the triggering of both somatic (physical) and affective (emotional) withdrawal symptoms during abstinence, which drive craving and maintain susceptibility to relapse [6]. Withdrawal symptoms associated with nicotine cessation are dependent on neuronal nicotinic acetylcholine receptors (nAChRs), which are upregulated and desensitized following chronic nicotine consumption [6–9]. Recent studies suggest that these adaptations result in reduced nAChR desensitization during abstinence, which enhances the sensitivity of the cholinergic system and can lead to altered neural circuit activity [6, 10]. It is therefore not surprising that neural circuits in which nAChRs are abundantly expressed play a key role during the onset and expression of nicotine withdrawal.

An important part of this neural circuitry is the medial habenula (MHb) to interpeduncular nucleus (IPN) pathway [11]. The MHb sends dense cholinergic projections to IPN neurons that are primarily GABAergic and project locally within the IPN and to other brain regions including the raphe nucleus and dorsolateral tegmentum [11]. Nicotinic AChRs are highly expressed along the MHb-IPN axis and previous studies have identified roles of various subtypes in nicotine reinforcement, aversion and both physical and affective symptoms of withdrawal [11–18]. Within the IPN, pharmacological and optogenetic manipulation of GABAergic activity has previously been shown to induce physical withdrawal symptoms including grooming, scratching, head shakes, and body tremors [18] in addition to inducing avoidance behavior [19]. However, it is not known if IPN GABAergic neuron activity is dynamically regulated during withdrawal as activity in vivo has not been measured, nor is it known whether increased somatic and affective behavior caused by nicotine withdrawal have functional consequences on IPN neural activity that is necessary for withdrawal behavior expression.

[1]Department of Neurobiology, Brudnick Neuropsychiatric Research Institute, University of Massachusetts Medical School, Worcester, MA, USA. [2]These authors contributed equally: Paul M. Klenowski, Rubing Zhao-Shea. ✉email: paul.klenowski@umassmed.edu; andrew.tapper@umassmed.edu

Received: 29 January 2021 Revised: 12 July 2021 Accepted: 13 July 2021
Published online: 29 July 2021

MATERIALS AND METHODS

Animals

All animal procedures were conducted in accordance with the guidelines for care and use of laboratory animals provided by the National Research Council, and with approved animal protocols from the Institutional Animal Care and Use Committee of the University of Massachusetts Medical School (UMMS). All experiments were performed using male mice that express Cre under the control of the glutamic acid decarboxylase-2 promoter (GAD2:Cre mice; stock# 010802) that were obtained from The Jackson Laboratory (West Grove, PA, USA). Mouse breeding was done at the UMMS animal facility. Cre lines were crossed with C57Bl/6J mice and only heterozygous animals were used for experiments. Mice were group housed with a maximum of five per cage and were kept on a standard 12 h light/dark cycle (light on at 7AM) and had access to standard chow and water ad libitum. Following viral injections, mice were given overnight to recover then switched to a reverse 12 h light/dark cycle (light on at 7PM) for at least 1 week prior to the start of experiments. All experiments were performed during the dark cycle.

Viral preparation

Plasmids pAAV-Ef1a-DIO-eNpHR3.0-eYFP and pAAV-Ef1a-DIO-eYFP were packaged into AAV serotype 2 (AAV2) viral particles at the UMMS Viral Vector Core. Viral titrations were 8.5×10^{12} genome copies per ml for pAAV-Ef1a-DIO-eNpHR3.0-eYFP and 5×10^{12} viral particles per ml for pAAV-Ef1a-DIO-eYFP. AAV-Flex-GCaMP6m packaged in AAV5 particles (pAAV.CAG.Flex.GCaMP6m.WPRE.SV40) was purchased from Addgene (100839-AAV5). Viral injections were performed 6 weeks before experiments to allow adequate time for transgene expression.

Viral injections

Male mice (6–8 weeks old) were deeply anaesthetized with a mixture of 100 mg/kg ketamine and 10 mg/kg xylazine (VEDCO), administered via intraperitoneal (IP) injection. Prior to surgery, the top of the skull was shaved and disinfected. Surgeries were performed using aseptic technique with the aid of a stereotaxic frame (Stoelting Co.). Mice were placed into the stereotaxic frame and the skull was exposed by making a small incision with a scalpel blade. Using bregma and lambda as landmarks, the skull was then leveled along the coronal and sagittal planes. A small drill hole was made in the skull that allowed injections to target the IPN. Microinjections were made using a Hamilton 10 µl neurosyringe (1701RN; Hamilton) and a microsyringe pump (Stoelting Co.) at the following coordinates (in mm, Bregma anterioposterior −3.51, mediolateral −1.0, dorsoventral 4.9 and 12° angle). Between 0.3 and 0.5 µl of virus was delivered through the syringe and at a constant flow rate of between 30 and 50 nl/min. After injection, the needle was left unmoved for 10 min before being slowly retracted. The incision was then closed and held together with glue.

Chronic nicotine and vehicle control treatment

Following viral injections, mice began 6 weeks of nicotine or vehicle control drinking. Nicotine or vehicle control solutions were prepared using nicotine hydrogen tartrate or L-tartaric acid (Sigma-Aldrich) dissolved in water at free base concentrations of 200 µg/ml. Each solution was sweetened by the addition of saccharin at a concentration of 3 mg/ml.

Implantation of optic fibers

Following 4 weeks of drinking, mice underwent surgery as described above for implantation of optic fibers. Optic fiber implants (200-µm core diameter; 0.48 NA, Doric Lenses) were targeted at the IPN (AP: −3.51, ML: −1.0, DV: −4.6, 12°) and were held in place using adhesive (C&B Metabond cement, Parkell Inc.) followed by dental cement (Cerebond, PlasticsOne). Following fiber implantation, mice drank nicotine or control solutions for an additional 2 weeks to complete the 6 weeks drinking protocol.

Post-surgery procedures

Following surgeries, mice were given time to recover from anesthesia in a cage with clean bedding placed on a heating pad. Mice received a subcutaneous injection of the analgesic ketoprofen (Zoetis; 1 mg/kg) and were monitored post-surgery until sternal. Mice were given a minimum of 1 week to recover from surgery before any experiments were performed. Following the completion of each experiment, mice were sacrificed by sodium pentobarbital overdose (200 mg/kg), perfused with 4% paraformaldehyde, and the brains were removed for verification of virus expression and fiber placement. Verification of viral expression and optic fiber placements was performed by experimenters blinded to behavioral outcome or treatment. Animals (<10%) with no viral expression, off-target viral expression, or misplaced optic fiber placement were excluded from analysis.

Mecamylamine-precipitated withdrawal

Following 6 weeks of nicotine or vehicle control drinking, mice were habituated to handling procedures and to IP saline injections for at least 3 days prior to the start of experiments. Mice then received an IP injection of either mecamylamine hydrochloride (1 mg/kg) dissolved in sterile saline or saline alone. Somatic withdrawal behaviors were scored in a manner similar to previous reports [18] by an observer that was blind to treatment. For optogenetic experiments, mice received nicotine via drinking water for 4 weeks after recovery from IPN injections of AAV2-DIO-eYFP or AAV2-DIO-NpHR 3.0 at age 6–8 weeks. Optic fibers were implanted as described above and mice received nicotine in their drinking water for an additional 2 weeks. Following 3 habituation IP injections of saline, mice received 1 mg/kg of mecamylamine or saline and were immediately put back into their home cage. Somatic signs that were scored included grooming, scratching, digging, body shaking, head nodding, backing, chewing, circling and jumping, which were tabulated once per event. Total time spent grooming, scratching, digging, and chewing was also determined. Analysis of somatic behavior was performed by an observer who was blind to the treatment conditions. Somatic behavior was recorded with a video camera for 20 min starting 2 min post-injection and optical inhibition occurred during the entire 20 min session. An LED and LED driver (Thorlabs) was used to deliver yellow light (593 nm, constant light 20 s on, 10 s off, ~15–20 mW output) in a manner identical to previous reports [20, 21].

Elevated plus maze

The elevated plus maze (EPM) apparatus consisted of a central junction (5 × 5 cm), four arms elevated 45 cm above the floor with each arm positioned at 90° relative to the adjacent arms. Two closed-arms were enclosed by high walls (30 × 5 × 15 cm) and the open-arms were exposed (30 × 5 × 0.25 cm). A 60 W red fluorescent light was positioned 100 cm above the maze and was used as an illumination source. Prior to being placed in the EPM chronic nicotine-treated GAD2:Cre mice expressing either NpHR or eYFP received 1 mg/kg of mecamylamine. Each mouse was then placed into the center part of the maze with their head facing one of the open-arms and was given 5 min of free exploration while having yellow light delivered into the IPN (593 nm, constant light 20 s on, 10 s off). The number of entries into the open- and closed-arms, and the total time spent in the open- and closed-arms were measured by MED-PC IV software (MED associates, Inc.) The time spent in open- and closed-arms was calculated as the standard anxiety indices. The total entries to open- and closed-arms were considered as the index of locomotor activity. The apparatus was cleaned thoroughly between trials. For photometry experiments, chronic nicotine-treated mice expressing GCaMP in the IPN were placed in the EPM for 5 min. Mice that underwent 48 h of spontaneous withdrawal had nicotine replaced with L-tartaric acid and were given a 5 min session in the EPM. Mice who completely avoided the open-arm in the first 5 min were given an additional 5 min in the EPM. All mice given a 10 min EPM exploration period entered the open-arm at least once. EPM exploration was recorded with a video camera and analyzed offline in a blinded fashion to determine time spent in the open- and closed-arms and total arm entries. All behavioral analysis was based on the first 5 min of EPM exploration. Photometry analysis included all data from the first 5 min of exploration and open-arm data from mice who were given an additional 5 min in the EPM.

Fiber photometry

GCaMP fluorescence was recorded with a Doric Instruments Fiber Photometry System. An LED driver was used to deliver excitation light from LEDs at 465 nm (~8.5 mW output) and at 405 nm (~5 mW output), which was used as an isosbestic wavelength for the indicator (Doric Instruments). The light was reflected into a 200 µm 0.48 N.A. optic fiber patch cord via the Dual Fluorescence Minicube (Doric Instruments). Emissions were detected with a femtowatt photoreceiver (Model 2151, Newport) and were amplified by transimpedance amplification to give an output voltage readout. The patch cord was connected to the optic fiber

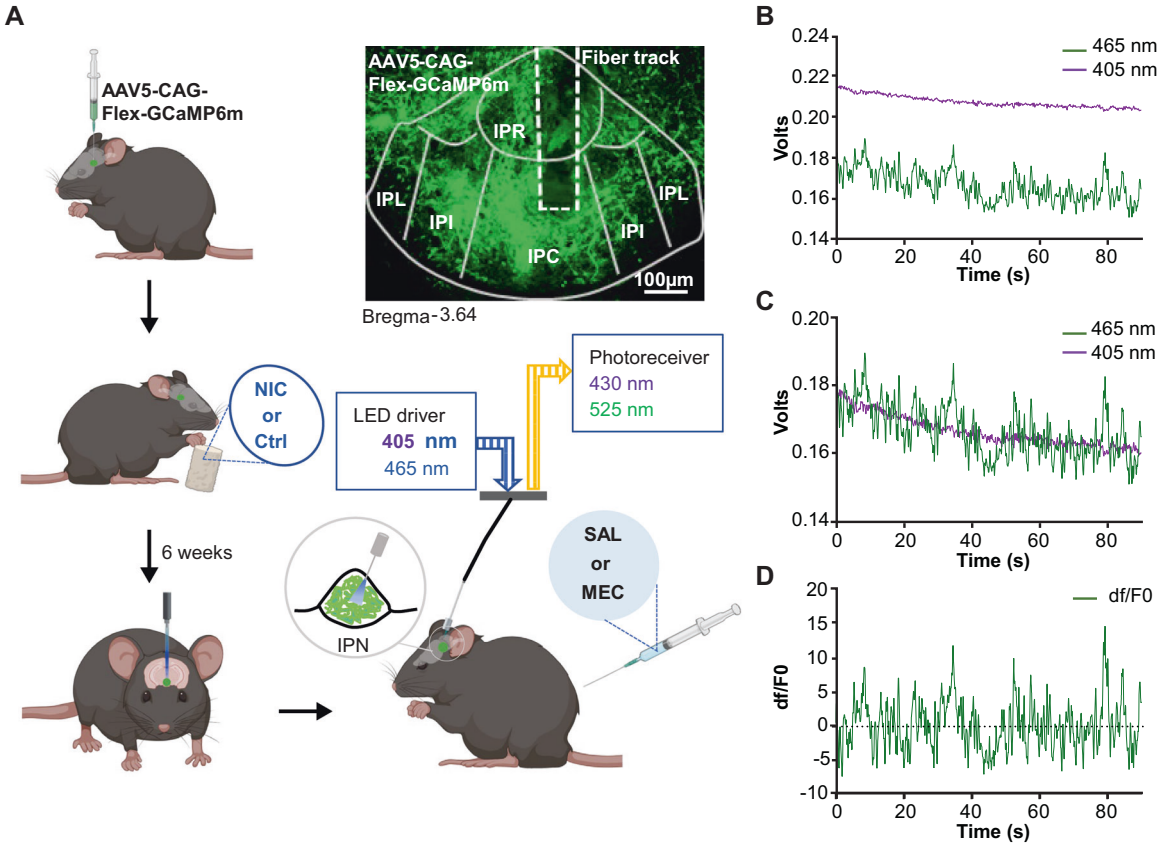

Fig. 1 Experimental design for combining GCaMP expression with fiber photometry to measure IPN GABAergic neuron activity during nicotine withdrawal. A Experimental design for recording GCaMP activity from GAD2:Cre IPN neurons during nicotine withdrawal. AAV5 Cre-dependent GCaMP6m was injected into the IPN of GAD2:Cre mice. Mice then received nicotine or vehicle control solution in their drinking water for 6 weeks. Mice had optic fibers implanted into the IPN 4–6 weeks following viral injections. Calcium dependent (465 nm) and independent (405 nm) fluorescence was then recorded following IP administration of mecamylamine (1 mg/kg) or saline. For analysis of photometry data, demodulated fluorescence signals **B** of the 405 nm channel were scaled to the 465 nm channel (**C**) using least mean squares linear regression. The scaled signals were used to calculate the dF/F_0 where dF/F_0 = (465 nm signal – fitted 405 nm signal)/fitted 405 nm signal (**D**) that were used for subsequent analysis. NIC nicotine, Ctrl control, MEC mecamylamine, SAL saline, IPR interpeduncular rostral, IPL interpeduncular lateral, IPI interpeduncular intermediate, IPC interpeduncular caudal.

implanted in the IPN prior to the start of the experiment. All recording sessions were performed within the home cage of each mouse. To determine the effects of mecamylamine on GCaMP activity, a baseline recording was made prior to injection. Chronic nicotine or control mice then received either a 1 mg/kg mecamylamine IP injection or saline injection and 1 min recordings were taken every 5 min post injection. Injections were counter-balanced so that half of the mice received mecamylamine first while the other half received an injection of saline first. To determine GCaMP signaling responses during somatic behaviors, chronic nicotine-treated mice were given 1 mg/kg mecamylamine or saline via IP injection. After mice were returned to their home cage, GCaMP fluorescence was recorded for 20 min post injection. To record somatic behaviors, a video camera was synchronized to the photometry system that time-locked the video and photometry recordings. Recordings were made for 20 min starting 2 min post injection. Somatic behavioral events were tallied from the videos in a blinded fashion and analysis was done using the time-locked photometry recording.

Fiber photometry analysis

Demodulated fluorescence signals were lowpass filtered (3 Hz) using the photometry analysis module of the Doric Neuroscience Studio software. Matlab scripts were used to scale the 405 nm channel to the 465 nm by applying a least mean squares linear regression and scaled signals were used to calculate the dF/F_0 where dF/F_0 = (465 nm signal – fitted 405 nm signal)/fitted 405 nm signal. Area under the curve (AUC) of the dF/F_0 curves was calculated in Graphpad Prism using the trapezoidal method. *Z*-scores were calculated using the average dF/F_0 values for each recording.

Statistical methods

Mean and standard error of the mean (SEM) were calculated for each data set. Where indicated, unpaired and paired Student's two-tailed *t*-tests, one-way ANOVAs with Sidak's post-tests, or two-way ANOVAs with Bonferroni's post-tests were conducted for all analyses involving the comparison of group means. AUC are shown as % changes in relation to baseline AUC measurements. *Z*-scores are presented mean ± SEM of all events for each somatic behavior. Comparisons of *z*-scores were made using the calculated average for each animal. All other data in the results and figures are presented as mean ± SEM. All analyses were performed using Prism 8 (Graphpad, San Diego, CA). Statistical significance was accepted at $P < 0.05$.

RESULTS

Mecamylamine-precipitated nicotine withdrawal increases IPN GABAergic neuron activity

To elucidate IPN GABAergic neuron activity in vivo in a mouse model of nicotine withdrawal, we used fiber photometry to record bulk calcium transients, a proxy for neuronal activity, measured as changes in fluorescence from a Cre-dependent genetically encoded calcium indicator, GCaMP6m [22], which was expressed in the IPN of GAD2:Cre mice via AAV5-mediated gene delivery. We recorded GCaMP fluorescence signal from GAD2:Cre IPN neurons in mice following 6 weeks of chronic nicotine drinking ($n = 7$), to elicit dependence, or vehicle control drinking ($n = 5$, Fig. 1A). Fluorescent signals from the 405 nm channel were scaled to the 465 nm channel prior to calculating the dF/F_0 for each recording

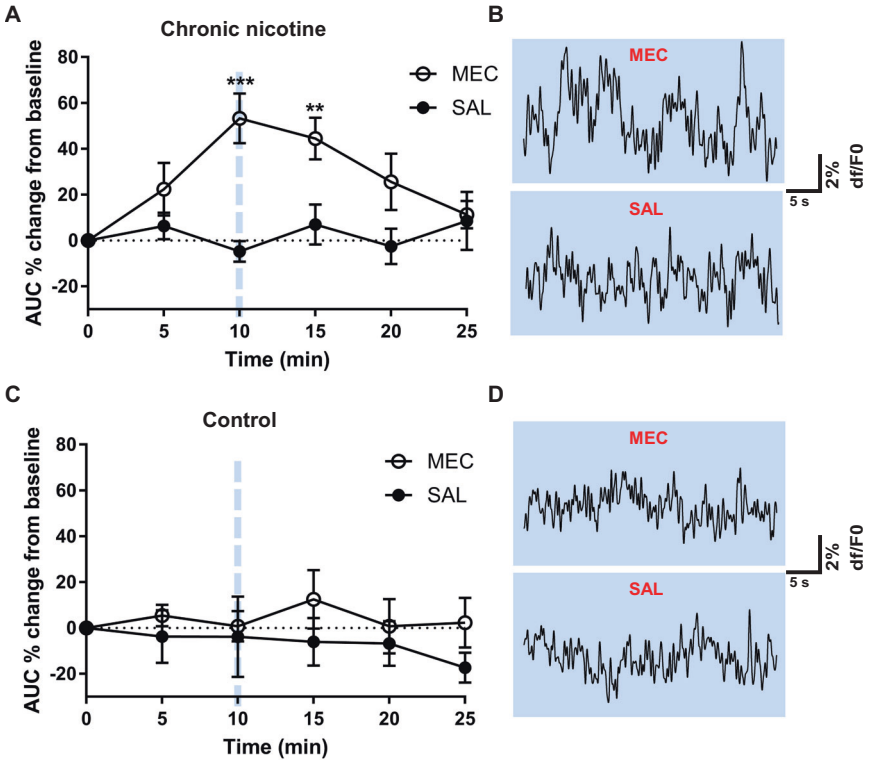

Fig. 2 Mecamylamine increases GCaMP activity from chronic nicotine but not vehicle control mice. Analysis of the effects of mecamylamine and saline injections on GCaMP activity in chronic nicotine and control mice. **A** In chronic nicotine-treated mice, mecamylamine (1 mg/kg) significantly increased the AUC of GCaMP recordings at 10 and 15 min post injection compared to baseline (two-way ANOVA with Bonferroni's post-tests). Representative GCaMP recordings taken 10 min post mecamylamine (top) and saline (bottom) injection are shown in (**B**). No significant differences in the AUC of GCaMP traces were observed in vehicle control mice following mecamylamine or saline injection (**C**). Representative traces for mecamylamine (top) and saline (bottom) from control mice are shown in (**D**). MEC mecamylamine, SAL saline.

(Fig. 1B–D). We then compared the AUC of baseline dF/F_0 recordings prior to injection to recordings following mecamylamine (1 mg/kg) or saline injections in nicotine-dependent or nicotine-naive control mice (Fig. 2). In nicotine-dependent mice (Fig. 2A, B), two-way ANOVA analysis revealed a significant time ($F_{(5,72)} = 2.54$, $P = 0.036$), drug ($F_{(1,72)} = 23.27$, $P < 0.0001$), and time × drug interaction ($F_{(5,72)} = 3.37$, $P = 0.009$). Post-tests revealed that mecamylamine significantly increased the AUC of GCaMP dF/F_0 traces recorded 10 min (53% ± 11%, $P = 0.0005$; Fig. 2A, B top) and 15 min (44% ± 9%, $P = 0.0066$; Fig. 2A) post injection compared to baseline (two-way ANOVA with Bonferroni's post-tests). The AUC of GCaMP recordings did not change at any time point compared to baseline following saline injection ($P >$ 0.9999, two-way ANOVA with Bonferroni's post-tests; Fig. 2A, B bottom). In nicotine-naive mice, no differences in GCaMP activity were observed following mecamylamine or saline injection ($P >$ 0.9999, two-way ANOVA with Bonferroni's post-tests; Fig. 2C, D). Virus expression and recording locations were confirmed in the IPN (Supplementary Fig. S1).

Somatic behaviors reduce IPN GABAergic neuron activity during mecamylamine-precipitated withdrawal

To test the response of somatic withdrawal symptoms on IPN GABAergic neuronal activity, we monitored GCaMP activity as above in a separate group of GAD2:Cre mice. Nicotine-dependent mice ($n = 13$) were injected with mecamylamine to induce somatic withdrawal or with saline as a control. In line with previous reports [18], mecamylamine precipitated significant increases in somatic withdrawal behaviors compared to after saline injection (Supplementary Fig. S2A). To determine GCaMP activity responses during somatic behaviors, we analyzed *z*-scores prior to onset and during somatic events. Based on previously reported kinetics of GCaMP6m [22], we focused our analysis on somatic behaviors that had an average duration of >2 s, to allow adequate time to capture changes to GCaMP fluorescence. This subset included grooming, scratching, digging, and chewing (Fig. 3). Somatic events were only included in the analysis if there were no other events that occurred in the 5 s prior to the event being analyzed. This reduced the likelihood that changes to the GCaMP signal were a result of any influence prior to the event being analyzed. We calculated the *z*-score for each event that met the above criteria (80% of somatic events post-saline and 72% of somatic events post-mecamylamine) and determined the average *z*-score of 1 s epochs starting 1 s prior to the event and ending 4 s following onset of the event. An average *z*-score of all events for each behavior per animal ($n = 9$–13) was used for comparative analysis. Time spent grooming ($t_{(12)} = 3.525$, $P = 0.0042$) and digging ($t_{(12)} = 6.251$, $P < 0.0001$) was significantly increased following mecamylamine compared to saline injection (Fig. 3A, B, paired Student's two-tailed *t*-test, $n = 13$). There was a trend to increased scratching ($t_{(12)} = 2.121$, $P = 0.0554$) and no difference in chewing time ($t_{(12)} = 1.084$, $P = 0.2997$) following mecamylamine vs saline injection (Fig. 3C, D, paired Student's two-tailed *t*-test, $n = 13$). Analysis of photometry recordings following mecamylamine challenge (Fig. 3E) revealed a significant decrease in the GCaMP signal during grooming events (average *z*-score per animal of 47 events; $n = 13$) that occurred in the 2–4 s period following onset compared to 1 s pre-onset (one-way ANOVA; $F_{(4,60)} = 3.25$, $P = 0.02$; post-tests, −1–0 s vs 2–3 s, $P = 0.02$, −1–0 s vs 3–4 s, $P = 0.03$, Fig. 3G). In contrast, no significant difference to GCaMP activity during grooming was detected following injection of saline (average *z*-score per animal of 28 events ($n = 9$), one-way

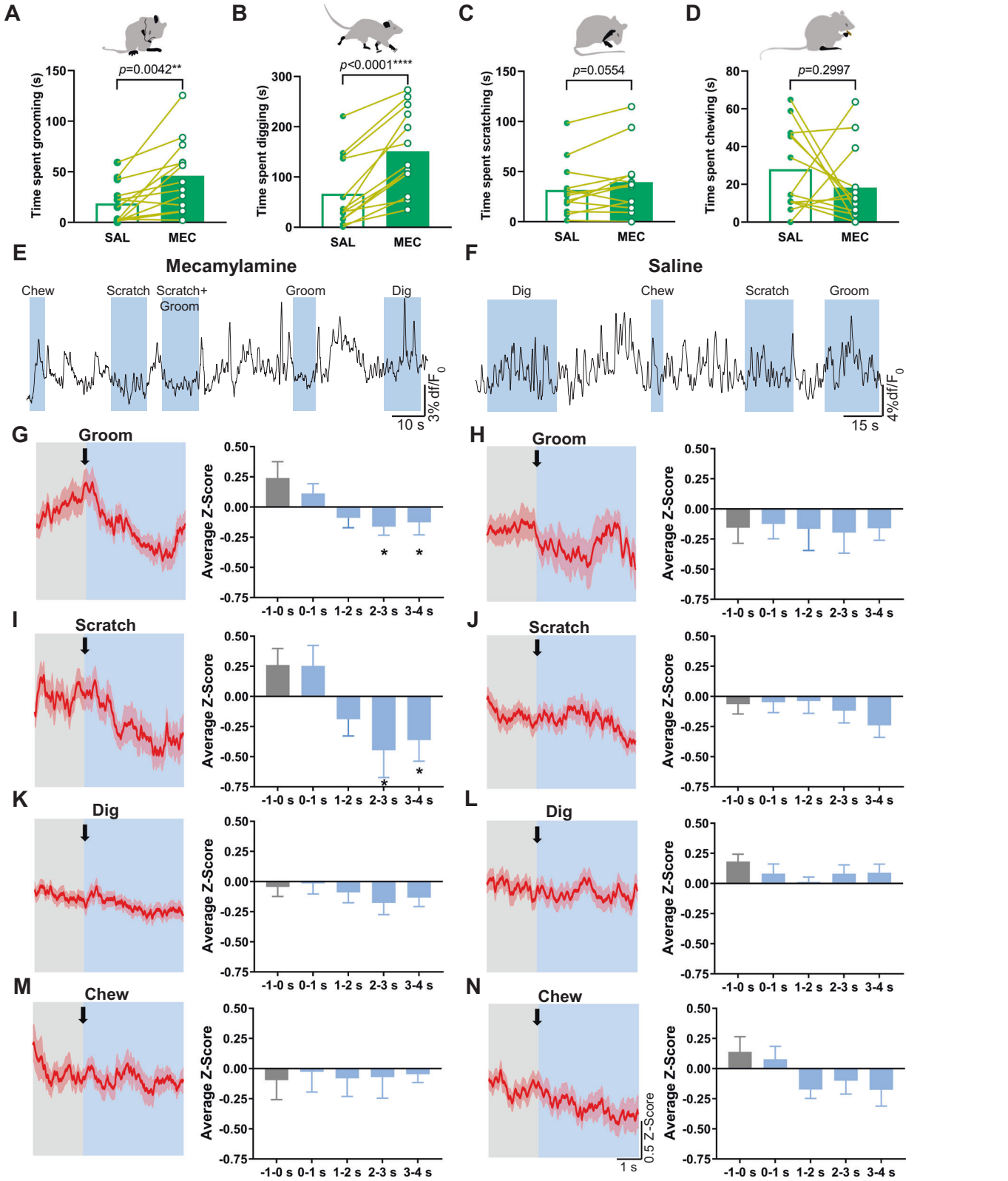

ANOVA; $F_{(4,39)} = 0.03$, $P = 0.99$, Fig. 3F, H). In addition, we found that scratching events after mecamylamine injection (average *z*-score per animal of 37 events; $n = 13$) significantly reduced the pre- vs post-onset GCaMP signal (one-way ANOVA; $F_{(4,58)} = 3.9$, $P < 0.001$; post-tests, −1–0 s vs 2–3 s, $P = 0.02$, −1–0 s vs 3–4 s, $P < 0.05$, Fig. 3E, I) but not following saline injection (average *z*-score per animal of 53 events ($n = 13$), one-way ANOVA; $F_{(4,65)} = 0.78$, $P = 0.54$, Fig. 3F, J). No significant difference in GCaMP activity was observed prior to the onset of digging events (average *z*-score per animal of 134 events for mecamylamine ($n = 13$) and 63 events for saline ($n = 13$), Fig. 3E, F, K, L) compared to post-onset following mecamylamine (one-way ANOVA; $F_{(4,65)} = 0.58$, $P = 0.68$) or saline

Fig. 3 Somatic behaviors reduce GCaMP signaling from IPN GAD2+ neurons during nicotine withdrawal. GCaMP responses were analyzed during bouts of somatic behaviors in nicotine-withdrawn mice and following saline injections. We focused our analysis on somatic behaviors that had an average duration of >2 s which included grooming, scratching, digging, and chewing. **A**–**D** Mecamylamine increased time spent grooming and digging in comparison to saline. There was also a trend to increased scratching time but no change in chewing time following mecamylamine vs saline administration. We recorded GCaMP activity of IPN GAD2+ neurons time-locked to somatic events following mecamylamine (**E**) and saline injection (**F**). *Z*-score plots were generated from all somatic events included in the analysis for grooming, scratching, digging, and chewing following mecamylamine (**G**, **I**, **K**, **M**) and saline injections (**H**, **J**, **L**, **N**). Plots show the *z*-scores from 2 s prior to the onset of each behavior (onset indicated by an arrow) until 4 s post onset. Comparisons were made using an average *z*-score per animal ($n = 9$–13) that was calculated from all events of each behavior. Following mecamylamine injection, we observed significant decreases in GCaMP activity 2–4 s post-onset of grooming compared to pre-onset (**G**). No significant difference in GCaMP activity pre- and post-onset of grooming occurred following saline injection (**H**). Significant reductions in GCaMP signaling were observed post-onset of scratching behavior compared to pre-onset following mecamylamine (**I**) but not saline injection (**J**). No difference in GCaMP activity was observed post-onset of digging and chewing events compared to pre-onset following mecamylamine (**K**, **M**) or saline injection (**L**, **N**). MEC mecamylamine, SAL saline.

injection (one-way ANOVA; $F_{(4,60)} = 0.82$, $P = 0.52$). In addition, no difference in GCaMP signal was detected prior to vs post-onset of chewing events (average *z*-score per animal of 31 events for mecamylamine ($n = 10$) and 40 events for saline ($n = 13$), Fig. 3E, F, M, N) in response to mecamylamine (one-way ANOVA; $F_{(4,50)} = 0.03$, $P = 0.997$) or saline (one-way ANOVA; $F_{(4,59)} = 1.71$, $P = 0.16$). Comparisons of differences in the *z*-scores pre-onset (–1–0 s) and post-onset (2–4 s) between treatment groups revealed that the somatic behaviors grooming and scratching significantly reduced GCaMP activity following mecamylamine as compared to saline injection (Supplementary Fig. S2B). No difference in pre- and post-onset GCaMP signal changes were detected between saline vs mecamylamine during digging and chewing behavior (Supplementary Fig. S2B). Virus expression and fiber locations were confirmed in the IPN (Supplementary Fig. S2C).

Optogenetic inhibition of GABAergic IPN neurons abolishes mecamylamine-induced increases in somatic withdrawal

Our photometry data indicate that there is an overall increase in IPN GABAergic activity in vivo during nicotine withdrawal. In addition, our results demonstrate that somatic behavior reduces GCaMP signaling within GAD2:Cre IPN neurons during nicotine withdrawal, possibly in an attempt to dynamically self-regulate activity. To investigate whether optogenetic silencing of IPN GABAergic activity could alleviate physical withdrawal signs, GAD2:Cre mice were IPN-injected with Cre-dependent NpHR or eYFP as a control using AAV2-mediated gene delivery as we have done previously [20, 21] and were given nicotine laced drinking water for 4 weeks. The mice then had optic fibers implanted and had additional 2 weeks of nicotine drinking to complete the 6 weeks drinking protocol (Fig. 4A). GAD2:Cre mice expressing NpHR ($n = 6$) or eYFP ($n = 7$) were administered mecamylamine or saline via IP injection and somatic signs were tallied during optical delivery of yellow light (593 nm) into the IPN (Fig. 4A). Following mecamylamine injection, eYFP mice exhibited a significant increase in somatic withdrawal signs compared to saline, which progressively increased and peaked between 10 and 15 min post mecamylamine administration (Fig. 4B), a time course in line with the observed increases of GCaMP activity recorded from IPN GAD2 + neurons (Fig. 2A). Two-way ANOVA analysis of total somatic behavior revealed a significant drug ($F_{(1,22)} = 20.03$, $P < 0.0001$), virus ($F_{(1,22)} = 24.25$, $P = 0.0002$) and drug × virus interaction ($F_{(1,22)} = 23.4$, $P < 0.0001$). Somatic behavioral events were increased in eYFP-expressing mice following mecamylamine compared to saline administration ($P < 0.0001$, two-way ANOVA with Bonferroni's post-tests, Fig. 4C), but this effect was not observed in NpHR-expressing mice ($P > 0.9999$, two-way ANOVA with Bonferroni's post-tests, Fig. 4C). No difference in somatic events were observed in eYFP compared to NpHR mice following saline injection ($P > 0.9999$, two-way ANOVA with Bonferroni's post-tests, Fig. 4C). Total somatic event time was also calculated for each behavior investigated in photometry experiments and was compared across groups and treatment conditions. Compared to saline, mecamylamine administration significantly increased time spent grooming ($P = 0.004$), scratching ($P = 0.004$), digging ($P < 0.05$) but not chewing ($P > 0.9999$) in eYFP mice (Fig. 4D, two-way ANOVA with Bonferroni's post-tests). NpHR mice did not exhibit significant differences in time spent grooming ($P > 0.9999$), scratching ($P > 0.9999$), digging ($P > 0.9999$), or chewing ($P > 0.9999$) following saline vs mecamylamine injection (Fig. 4D, two-way ANOVA with Bonferroni's post-tests). Saline injection did not change time spent grooming ($P > 0.9999$), scratching ($P > 0.9999$), digging ($P > 0.9999$), or chewing in eYFP compared to NpHR mice (Fig. 4D, two-way ANOVA with Bonferroni's post-tests). These data show that optical silencing of GAD2+ IPN neurons inhibited the expression of physical withdrawal symptoms precipitated by mecamylamine. Virus expression and fiber placements were verified within the IPN (Supplementary Fig. S3).

Increased IPN GABAergic activity contributes to anxiety-like behavior during nicotine withdrawal

Because previous studies have implicated the MHb-IPN pathway in the anxiogenic effects of nicotine withdrawal [17], we utilized the EPM to determine whether IPN GABAergic neuron activity is involved in withdrawal-induced anxiety-like behavior. EPM photometry experiments were performed with chronic nicotine-treated mice prior to and following a spontaneous 48 h withdrawal (Fig. 5A). Nicotine withdrawal increased anxiety-like behavior as evidenced by significantly reduced time spent in the open-arms ($t_{(6)} = 3.685$, $P = 0.01$) and increased time in closed-arms ($t_{(6)} = 3.072$, $P = 0.02$) compared to when mice were not in withdrawal (Fig. 5B, C, paired Student's two-tailed *t*-test). No difference in total arm entries were observed in withdrawn vs non-withdrawn mice ($t_{(6)} = 0.3073$, $P = 0.77$) suggesting that this result was not due to changes in locomotor activity (Fig. 5D, paired Student's two-tailed *t*-test). We then compared the activity of IPN GAD2+ neurons during closed- vs open-arm exploration. Interestingly, prior to withdrawal, no difference in GCaMP activity was observed when mice explored the closed- or open-arms ($t_{(6)} = 1.867$, $P = 0.11$, paired Student's two-tailed *t*-test, Fig. 5E, F); however, following 48 h withdrawal, open-arm exploration significantly enhanced the GCaMP signal from IPN GAD2+ neurons compared to when mice were in the closed-arms ($t_{(6)} = 2.821$, $P = 0.03$, paired Student's two-tailed *t*-test, Fig. 5G, H). Following mecamylamine challenge, optical inhibition of IPN GAD2+ neurons in NpHR mice increased open-arm exploration ($t_{(10)} = 2.288$, $P < 0.05$) and reduced time spent in the closed-arms ($t_{(10)} = 2.373$, $P = 0.04$) compared to eYFP mice (unpaired Student's two-tailed *t*-test, Fig. 5I, J). Total arm entries were not different between the groups ($t_{(10)} = 1.852$, $P = 0.09$, paired Student's two-tailed *t*-test, Fig. 5K). These results suggest that nicotine withdrawal can sensitize activation of IPN GABAergic neurons during open-arm exploration in the EPM, which increases avoidance and contributes to the anxiogenic

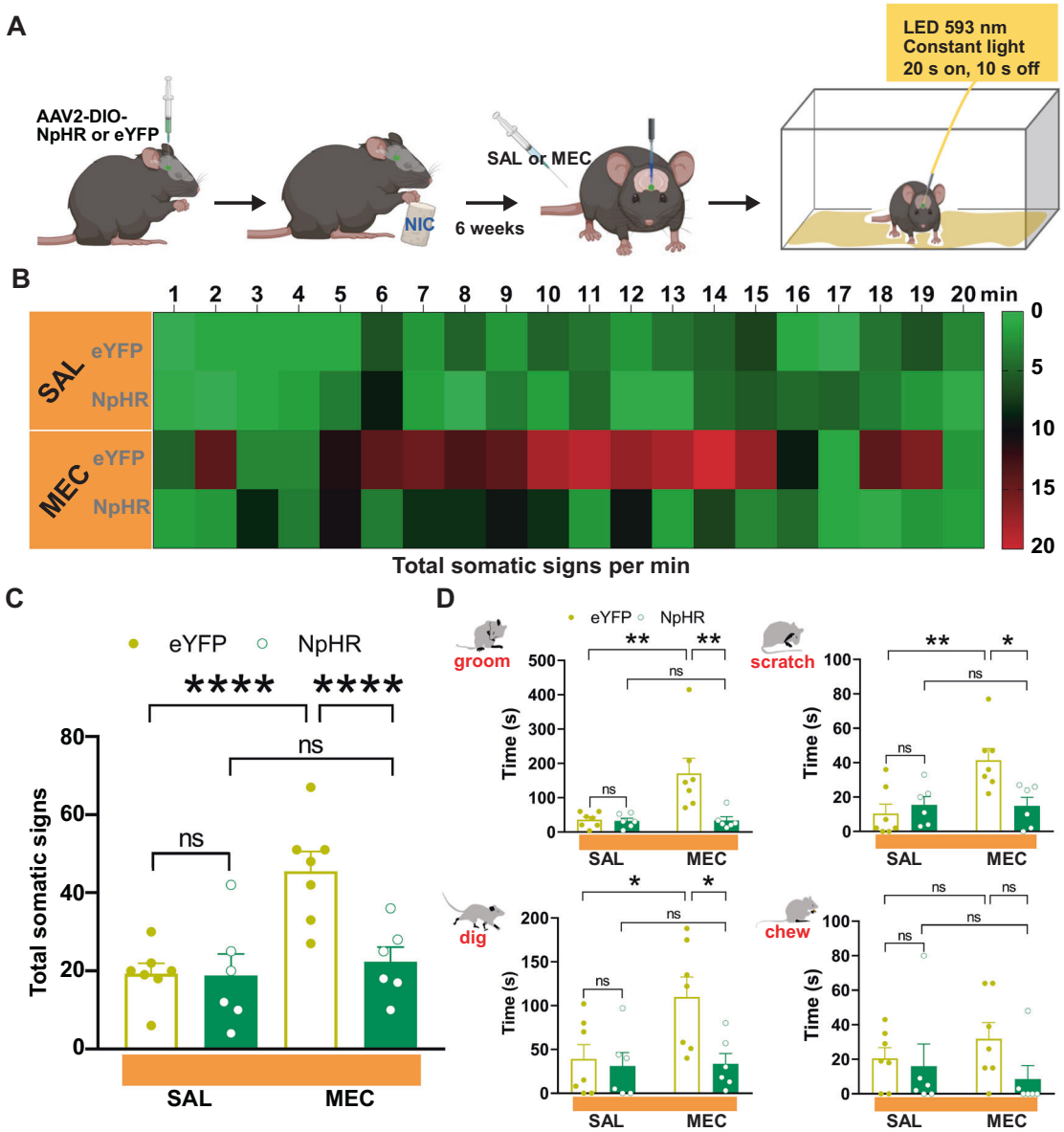

Fig. 4 Physical signs of nicotine withdrawal are inhibited by optical silencing of IPN GAD2+ neurons. A Experimental design for optical silencing of IPN GAD2+ neurons. AAV2 Cre-dependent NpHR or eYFP were injected into the IPN of GAD2:Cre mice. Following 6 weeks of chronic nicotine drinking and implantation of optic fibers, mice were challenged with mecamylamine or saline in the presence of yellow light (593 nm, 20 s on, 10 s off) delivered into the IPN. Following injections, mice were immediately returned to their home cage and somatic behaviors were tallied for 20 min starting 2 min post injection. Time course of somatic events per min under each condition is shown in the heatmap in (**B**). Heatmap legend indicates number of somatic events. **C** In eYFP-expressing mice, mecamylamine induced a significant increase in somatic behavioral events as compared to saline, while no difference in total somatic behavior was observed following mecamylamine challenge compared to saline in NpHR-expressing mice (two-way ANOVA with Bonferroni's post-tests). Total somatic event time was also calculated for each behavior investigated in photometry experiments and was compared across groups and treatment conditions. **D** Significant increases in time spent grooming, scratching, and digging were observed following mecamylamine injection as compared to saline in eYFP mice, but not NpHR-expressing mice (two-way ANOVA with Bonferroni's post-tests). No difference in chewing time was observed across groups or treatment conditions (two-way ANOVA with Bonferroni's post-tests). MEC mecamylamine, SAL saline.

effect of nicotine withdrawal. All virus and fiber placements were verified within the IPN (Supplementary Fig. S4).

DISCUSSION

The symptoms of nicotine withdrawal are emotional and physical barriers that prevent chronic nicotine users from self-limiting their intake despite negative consequences [1, 6]. The expression of affective and physical withdrawal symptoms during abstinence also drives craving and increases vulnerability to relapse [23]. These can include affective symptoms such as anxiety, stress, irritability, and anhedonia, as well as physical symptoms including tremors, bradycardia, gastrointestinal pain, and raised appetite [11]. In mice, physical symptoms associated with nicotine withdrawal include grooming, scratching, digging, body shakes, head nodding, backing, and chewing [11, 24]. Previous studies have identified the MHb-IPN circuit as being critically involved in the initiation and expression of somatic and affective symptoms during nicotine withdrawal [16, 18, 25]. However, data suggesting activation of IPN GABAergic neurons during nicotine withdrawal

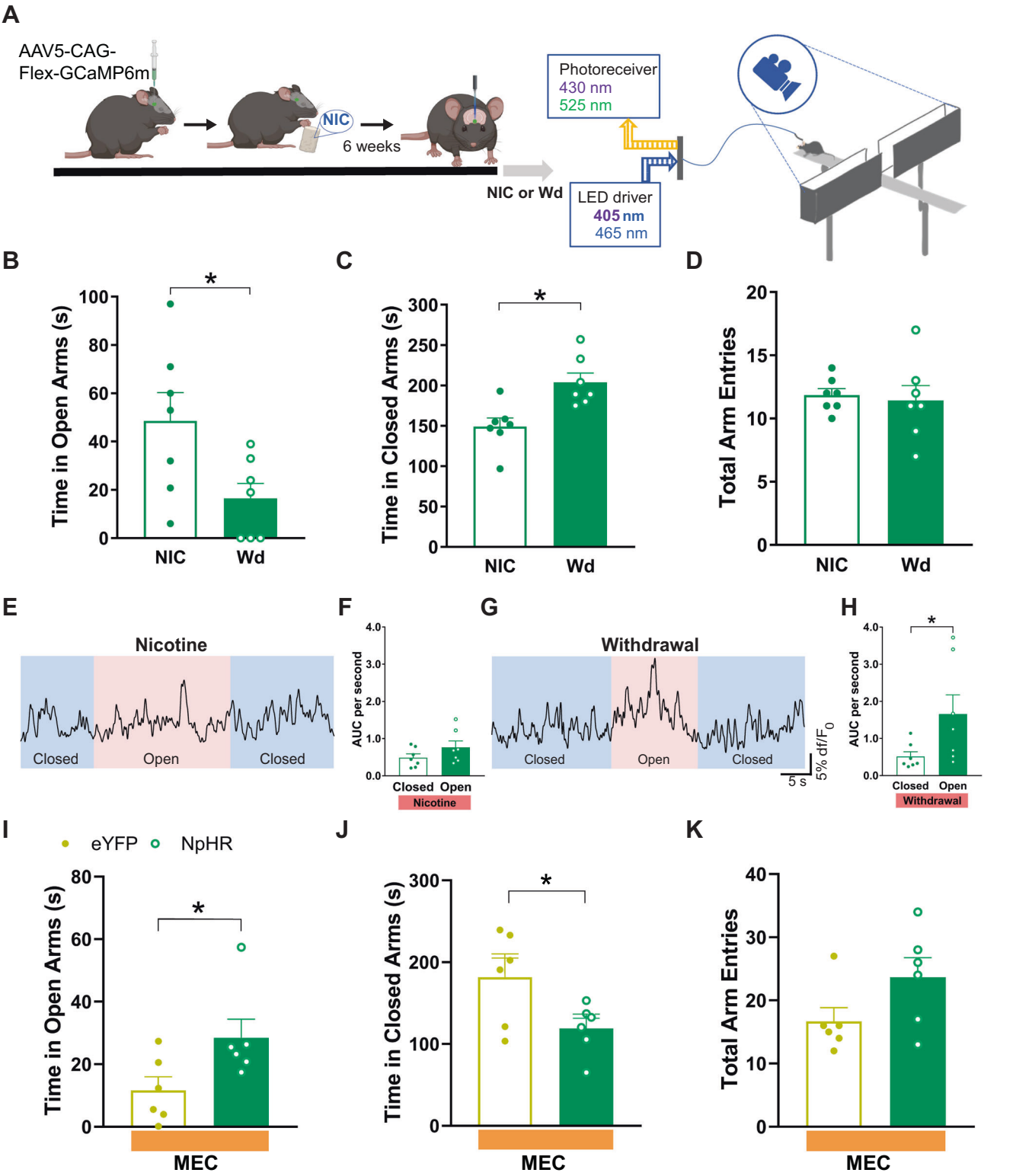

Fig. 5 Activation of IPN GABAergic neurons during withdrawal controls anxiety-like avoidance of open-arm exploration in the elevated plus maze. A To record GCaMP responses during EPM exploration, GAD2:Cre mice had GCaMP and optic fibers implanted into the IPN and underwent 6 weeks of chronic nicotine treatment. Behavior in the EPM was recorded prior to and following 48 h spontaneous withdrawal from nicotine. **B**–**D** Mice in withdrawal significantly decreased open-arm exploration and increased time spent in the closed-arms but did not change total arm entries compared to when they were not in withdrawal. Prior to withdrawal, GCaMP activity did not change in the closed- (blue shaded **E**) vs open-arm (pink shaded **E**, **F**), whereas a significant increase in GCaMP signal was observed during exploration of the open-arm (pink shaded **G**) compared to the closed-arm (blue shaded **G**) when mice were in nicotine withdrawal (**H**). Optical silencing of IPN GAD2+ neurons in NpHR mice significantly increased time spent in the open-arms compared to eYFP mice following mecamylamine challenge and reduced time spent in the closed-arms (**I**, **J**). Total arm entries were not different between NpHR and eYFP mice (**K**). NIC chronic nicotine, Wd 48 h nicotine withdrawal, MEC mecamylamine, SAL saline.

[18] utilized c-fos immunoreactivity as a marker of neuronal activation ex vivo and found that mecamylamine increased c-fos expression in IPN GABAergic neurons from nicotine-dependent mice compared to nicotine-naive mice, an observation that has since been repeated by other groups [26, 27]. In addition, IPN infusion of the glutamate receptor antagonist AP5 prior to infusion of mecamylamine significantly reduced c-fos expression and somatic behavior suggesting that glutamate release, presumably from MHb inputs, is required for the expression of the physical and affective symptoms of nicotine withdrawal [17, 18]. We have extended these studies by investigating in vivo responses of IPN GABAergic neurons during nicotine withdrawal that, to our knowledge, have not been reported previously. Our real-time analysis of GCaMP signaling detected significant increases in IPN GABAergic excitability during nicotine withdrawal. In addition, we found that open-arm exploration increased the activity of IPN GAD2+ neurons specifically during withdrawal. We also identified somatic behavioral responses that reduce IPN GABAergic activity in withdrawal.

Our data raise the question as to how IPN GABAergic neuronal activity is heightened and why behavioral effects on IPN neural activity only emerge during periods of nicotine withdrawal. Previous studies suggest that chronic nicotine upregulates nAChRs within the MHb-IPN pathway, perhaps in response to desensitization, which could lead to increased nicotinic signaling and neural circuit activity during withdrawal [6, 10, 28]. As the MHb-IPN circuit has previously been implicated in fear [29], anxiety, and avoidance [19], as well as novelty seeking [21], it is possible that sensitization of the MHb-IPN circuit during nicotine withdrawal contributed to enhanced activation of IPN GABAergic neurons during open-arm exploration, leading to increased avoidance behavior and decreased novelty seeking. In addition, increased IPN GABAergic activity likely drives increased somatic behavior as a withdrawal-coping mechanism (as discussed below).

During negative emotional states, somatic behavioral responses such as grooming and scratching may be associated with rewarding or positive valence due to their ability to support stress reduction and improve sense of well-being [30–33]. Supporting this idea, previous studies indicate that optogenetic activation of IPN neurons is aversive, while we have previously implicated increased IPN neuron activation in increased expression of somatic and anxiety-like behavior especially during nicotine withdrawal [17, 19]. In line with these studies, we found that inhibiting IPN GABAergic neurons reduced withdrawal-induced increases in somatic and anxiety-like behavior. Thus, our data support the hypothesis that grooming and scratching behavior is driven by increased activity of IPN GABAergic neurons as a withdrawal-coping mechanism and demonstrate a site of action where grooming and scratching can directly influence/reduce neural activity and reverse effects of nicotine withdrawal. Interestingly, we found that completion of grooming events generally led to a rebound excitation of the GCaMP signal. This could explain why a ramp up in GCaMP activity was often observed prior to the onset of grooming. Whether or not this contributed to the sustained increase in grooming behavior during withdrawal requires further investigation.

Negative emotional states can cause harmful effects from sustained periods of heightened stress [34, 35]. Therefore, behavioral adaptations that displace stress activity can protect against damage from exaggerated responses and improve well-being [32]. Although the mechanisms that underlie these effects have not been fully elucidated, we identified significant reductions in GCaMP signaling from IPN GAD2+ neurons that occurred following the onset of grooming or scratching events. This suggests that during these behaviors, specific changes in the excitability of GAD2+ IPN neurons occur during nicotine withdrawal that are not observed from other somatic signs including digging and chewing. Previous studies have shown that IPN GAD2+ excitability is controlled by local interneurons that exhibit discrete localization and protein expression [18, 36]. In addition, GABAergic IPN neurons receive dense innervation from the MHb that provides the main source of glutamate as well as acetylcholine to the IPN [37, 38]. Anatomical evidence also suggests that the IPN is sparsely innervated by the prefrontal cortex [39], hypothalamus [40], and raphe nuclei [41]. Currently, there is no clear evidence to suggest that direct afferent IPN connections respond to innate motor behaviors such as grooming and scratching. This is not surprising given the fact that these real-time behavioral responses were only detected in mice undergoing nicotine withdrawal. However, it is possible that IPN inputs could be modulated via upstream projections that have not yet been determined. For example, previous studies have identified brain areas that initiate and control patterns of motor behaviors such as grooming [31, 42]. Efferent outputs from the hypothalamus that evoke self-grooming in rodents project to various parts of the limbic system including the septum, medial amygdala, and ventral tegmental area [42]. Downstream effects from these projections may influence neural activity within the IPN. Specifically, efferent fibers from the hypothalamus that initiate grooming responses project to septum that in turn innervates MHb via projections from the triangular septal nucleus [43] and medial septum [44]. However, the septum also receives hypothalamic input that is not involved in grooming responses; therefore, additional anatomical evidence is required in order to implicate this pathway in the grooming effects observed in our study. Hypothalamic efferent projections that initiate grooming also innervate the preoptic nucleus [42] and the IPN receives afferents from this area [45], which could provide another possible source of inhibitory input. In addition, VTA dopamine neurons are another location upstream from the IPN that receive hypothalamic inputs that facilitate grooming, in addition to afferents that are involved in itch-induced scratching behavior [42, 46]. A recently described VTA-IPN connection could provide a convergent site where grooming and scratching responses may act to modulate IPN GABAergic activity [20]. While this study observed inhibitory and excitatory responses to dopamine on IPN GABAergic activity, it is not known whether chronic nicotine treatment can shift the balance of inhibition and excitation within this pathway and contribute to the effects of grooming and scratching during withdrawal.

Because negative emotional states including stress, anxiety, and nicotine withdrawal can increase grooming and scratching behavior [31, 36, 47], it has been hypothesized that these behavioral responses provide hedonic value. This is supported by studies that have identified connections between brain regions that control scratching and grooming behavior and the VTA, changes in the activity of VTA dopamine neurons during itch-induced scratching, and changes in grooming and scratching responses following the administration of drugs that modulate dopamine receptor activity [30, 31]. Although it is possible that grooming and scratching may activate the mesolimbic dopamine pathway during nicotine withdrawal causing dopamine release into the IPN that could lead to reduced GABAergic activity, influences by other IPN afferents or local neuromodulators cannot be ruled out since optogenetic silencing of GABAergic IPN neurons completely inhibited the expression of mecamylamine-precipitated somatic withdrawal. One would also expect inhibition of IPN GABAergic neurons to alter activity in downstream projections areas. This could explain why digging behavior does not influence GABAergic activity within the IPN but is controlled by modulating IPN GABAergic neurons. A possible downstream target involved in controlling digging behavior is the raphe nucleus that receives GABAergic input from the IPN [11]. Modulation of serotonergic synaptic transmission has been widely implicated in previous studies of anxiety and repetitive digging associated with marble burying [48]. The identification of novel

molecular mechanisms that inhibit the activity of the MHb-IPN pathway to reduce symptoms of nicotine withdrawal could lead to the development of improved treatment options for the management of nicotine addiction.

REFERENCES

1. Prochaska JJ, Benowitz NL. Current advances in research in treatment and recovery: nicotine addiction. Sci Adv. 2019;5:eaay9763.
2. Stolerman IP, Jarvis MJ. The scientific case that nicotine is addictive. Psychopharmacol (Berl). 1995;117:2–10. discussion 4–20.
3. Office of the Surgeon General. The Health Consequences of Smoking-50 Years of Progress: A Report of the Surgeon General. Reports of the Surgeon General. Centers for Disease Control and Prevention. Atlanta, 2014.
4. The Federal Trade Commission. Federal Trade Commission Cigarette Report for 2018. Washington. https://www.ftc.gov/system/files/documents/reports/federal-trade-commission-cigarette-report-2018-smokeless-tobacco-report-2018/p114508cigarettereport2018.pdf.
5. Jha P, Ramasundarahettige C, Landsman V, Rostron B, Thun M, Anderson RN, et al. 21st-century hazards of smoking and benefits of cessation in the United States. N Engl J Med. 2013;368:341–50.
6. McLaughlin I, Dani JA, De Biasi M. Nicotine withdrawal. Curr Top Behav Neurosci. 2015;24:99–123.
7. Fowler CD, Arends MA, Kenny PJ. Subtypes of nicotinic acetylcholine receptors in nicotine reward, dependence, and withdrawal: evidence from genetically modified mice. Behav Pharm. 2008;19:461–84.
8. Brunzell DH, Stafford AM, Dixon CI. Nicotinic receptor contributions to smoking: insights from human studies and animal models. Curr Addict Rep. 2015;2:33–46.
9. Nashmi R, Xiao C, Deshpande P, McKinney S, Grady SR, Whiteaker P, et al. Chronic nicotine cell specifically upregulates functional alpha 4* nicotinic receptors: basis for both tolerance in midbrain and enhanced long-term potentiation in perforant path. J Neurosci. 2007;27:8202–18.
10. Klenowski PM, Tapper AR. Molecular, neuronal, and behavioral effects of ethanol and nicotine interactions. Handb Exp Pharm. 2018;248:187–212.
11. Antolin-Fontes B, Ables JL, Gorlich A, Ibanez-Tallon I. The habenulo-interpeduncular pathway in nicotine aversion and withdrawal. Neuropharmacology. 2015;96:213–22.
12. Fowler CD, Kenny PJ. Nicotine aversion: neurobiological mechanisms and relevance to tobacco dependence vulnerability. Neuropharmacology. 2014;76:533–44.
13. Fowler CD, Lu Q, Johnson PM, Marks MJ, Kenny PJ. Habenular alpha5 nicotinic receptor subunit signalling controls nicotine intake. Nature. 2011;471:597–601.
14. Frahm S, Slimak MA, Ferrarese L, Santos-Torres J, Antolin-Fontes B, Auer S, et al. Aversion to nicotine is regulated by the balanced activity of beta4 and alpha5 nicotinic receptor subunits in the medial habenula. Neuron. 2011;70:522–35.
15. Harrington L, Vinals X, Herrera-Solis A, Flores A, Morel C, Tolu S, et al. Role of beta4* nicotinic acetylcholine receptors in the habenulo-interpeduncular pathway in nicotine reinforcement in mice. Neuropsychopharmacology. 2016;41:1790–802.
16. Salas R, Sturm R, Boulter J, De Biasi M. Nicotinic receptors in the habenulo-interpeduncular system are necessary for nicotine withdrawal in mice. J Neurosci. 2009;29:3014–8.
17. Zhao-Shea R, DeGroot SR, Liu L, Vallaster M, Pang X, Su Q, et al. Increased CRF signalling in a ventral tegmental area-interpeduncular nucleus-medial habenula circuit induces anxiety during nicotine withdrawal. Nat Commun. 2015;6:6770.
18. Zhao-Shea R, Liu L, Pang X, Gardner PD, Tapper AR. Activation of GABAergic neurons in the interpeduncular nucleus triggers physical nicotine withdrawal symptoms. Curr Biol. 2013;23:2327–35.
19. Wolfman SL, Gill DF, Bogdanic F, Long K, Al-Hasani R, McCall JG, et al. Nicotine aversion is mediated by GABAergic interpeduncular nucleus inputs to laterodorsal tegmentum. Nat Commun. 2018;9:2710.
20. DeGroot SR, Zhao-Shea R, Chung L, Klenowski PM, Sun F, Molas S, et al. Midbrain dopamine controls anxiety-like behavior by engaging unique interpeduncular nucleus microcircuitry. Biol Psychiatry. 2020;88:855–66.
21. Molas S, Zhao-Shea R, Liu L, DeGroot SR, Gardner PD, Tapper AR. A circuit-based mechanism underlying familiarity signaling and the preference for novelty. Nat Neurosci. 2017;20:1260–8.
22. Chen TW, Wardill TJ, Sun Y, Pulver SR, Renninger SL, Baohan A, et al. Ultrasensitive fluorescent proteins for imaging neuronal activity. Nature. 2013;499:295–300.
23. Robinson JD, Li L, Chen M, Lerman C, Tyndale RF, Schnoll RA, et al. Evaluating the temporal relationships between withdrawal symptoms and smoking relapse. Psychol Addict Behav. 2019;33:105–16.
24. Damaj MI, Kao W, Martin BR. Characterization of spontaneous and precipitated nicotine withdrawal in the mouse. J Pharm Exp Ther. 2003;307:526–34.
25. Correa VL, Flores RJ, Carcoba LM, Arreguin MC, O'Dell LE. Sex differences in cholinergic systems in the interpeduncular nucleus following nicotine exposure and withdrawal. Neuropharmacology. 2019;158:107714.
26. Shih PY, Engle SE, Oh G, Deshpande P, Puskar NL, Lester HA, et al. Differential expression and function of nicotinic acetylcholine receptors in subdivisions of medial habenula. J Neurosci. 2014;34:9789–802.
27. Upton M, Lotfipour S. alpha2-Null mutant mice have altered levels of neuronal activity in restricted midbrain and limbic brain regions during nicotine withdrawal as demonstrated by cfos expression. Biochem Pharm. 2015;97:558–65.
28. Arvin MC, Jin XT, Yan Y, Wang Y, Ramsey MD, Kim VJ, et al. Chronic nicotine exposure alters the neurophysiology of habenulo-interpeduncular circuitry. J Neurosci. 2019;39:4268–81.
29. Zhang J, Tan L, Ren Y, Liang J, Lin R, Feng Q, et al. Presynaptic excitation via GABAB receptors in habenula cholinergic neurons regulates fear memory expression. Cell. 2016;166:716–28.
30. Chen XJ, Sun YG. Central circuit mechanisms of itch. Nat Commun. 2020;11:3052.
31. Kalueff AV, Stewart AM, Song C, Berridge KC, Graybiel AM, Fentress JC. Neurobiology of rodent self-grooming and its value for translational neuroscience. Nat Rev Neurosci. 2016;17:45–59.
32. Mu MD, Geng HY, Rong KL, Peng RC, Wang ST, Geng LT, et al. A limbic circuitry involved in emotional stress-induced grooming. Nat Commun. 2020;11:2261.
33. Sanders KM, Sakai K, Henry TD, Hashimoto T, Akiyama T. A subpopulation of amygdala neurons mediates the affective component of itch. J Neurosci. 2019;39:3345–56.
34. Charmandari E, Tsigos C, Chrousos G. Endocrinology of the stress response. Annu Rev Physiol. 2005;67:259–84.
35. Weston CS. Posttraumatic stress disorder: a theoretical model of the hyperarousal subtype. Front Psychiatry. 2014;5:37.
36. Ables JL, Gorlich A, Antolin-Fontes B, Wang C, Lipford SM, Riad MH, et al. Retrograde inhibition by a specific subset of interpeduncular alpha5 nicotinic neurons regulates nicotine preference. Proc Natl Acad Sci USA. 2017;114:13012–7.
37. Herkenham M, Nauta WJ. Efferent connections of the habenular nuclei in the rat. J Comp Neurol. 1979;187:19–47.
38. Ren J, Qin C, Hu F, Tan J, Qiu L, Zhao S, et al. Habenula "cholinergic" neurons co-release glutamate and acetylcholine and activate postsynaptic neurons via distinct transmission modes. Neuron. 2011;69:445–52.
39. Takagishi M, Chiba T. Efferent projections of the infralimbic (area 25) region of the medial prefrontal cortex in the rat: an anterograde tracer PHA-L study. Brain Res. 1991;566:26–39.
40. Hamill GS, Jacobowitz DM. A study of afferent projections to the rat interpeduncular nucleus. Brain Res Bull. 1984;13:527–39.
41. Conrad LC, Leonard CM, Pfaff DW. Connections of the median and dorsal raphe nuclei in the rat: an autoradiographic and degeneration study. J Comp Neurol. 1974;156:179–205.
42. Roeling TA, Veening JG, Peters JP, Vermelis ME, Nieuwenhuys R. Efferent connections of the hypothalamic "grooming area" in the rat. Neuroscience. 1993;56:199–225.
43. Herkenham M, Nauta WJ. Afferent connections of the habenular nuclei in the rat. A horseradish peroxidase study, with a note on the fiber-of-passage problem. J Comp Neurol. 1977;173:123–46.
44. Qin C, Luo M. Neurochemical phenotypes of the afferent and efferent projections of the mouse medial habenula. Neuroscience. 2009;161:827–37.
45. Shibata H, Suzuki T, Matsushita M. Afferent projections to the interpeduncular nucleus in the rat, as studied by retrograde and anterograde transport of wheat germ agglutinin conjugated to horseradish peroxidase. J Comp Neurol. 1986;248:272–84.
46. Su XY, Chen M, Yuan Y, Li Y, Guo SS, Luo HQ, et al. Central processing of itch in the midbrain reward center. Neuron. 2019;102:858–72.
47. Sanders KM, Akiyama T. The vicious cycle of itch and anxiety. Neurosci Biobehav Rev. 2018;87:17–26.
48. de Brouwer G, Fick A, Harvey BH, Wolmarans W. A critical inquiry into marble-burying as a preclinical screening paradigm of relevance for anxiety and obsessive-compulsive disorder: mapping the way forward. Cogn Affect Behav Neurosci. 2019;19:1–39.

ACKNOWLEDGEMENTS

We thank Anthony Sacino for technical support, Karl Deisseroth for optogenetic plasmids, and Biorender.com for use of graphics. The content is solely the responsibility of the authors and does not necessarily represent the official views of the National Institutes of Health.

AUTHOR CONTRIBUTIONS

PMK, RZ-S, and ART conceived the study. PMK, RZ-S, and SM performed experiments. PMK, RZ-S, and TGF analyzed data. PMK, RZ-S, and ART interpreted the data. PMK and ART wrote the manuscript with input from the other authors.

FUNDING AND DISCLOSURE

This work was supported by the National Institute on Drug Abuse award numbers DA041482 (ART), DA047678 (ART) and by the Brudnick Fellowship in Mood Disorders (PMK). All authors report no competing financial interests or potential conflicts of interest.

ADDITIONAL INFORMATION

Supplementary information The online version contains supplementary material available at https://doi.org/10.1038/s41386-021-01107-1.

Correspondence and requests for materials should be addressed to P.M.K. or A.R.T.